

1 **Social Behaviour and Collective Motion in Plant-Animal Worms.**

2 Nigel R. Franks^{1*}, Alan Worley¹, Katherine A.J. Grant¹, Alice R. Gorman¹, Victoria
3 Vizard¹, Harriet Plackett¹, Carolina Doran¹, Margaret L. Gamble¹, Martin C. Stumpe²,
4 Ana B. Sendova-Franks³

5 ¹School of Biological Sciences, University of Bristol, UK

6 ²AnTracks Computer Vision Systems, Mountain View, CA, USA

7 ³Department of Engineering Design and Mathematics, UWE, Bristol, UK

8 *corresponding author email: nigel.franks@bristol.ac.uk

9 **Abstract**

10 Social behaviour may enable organisms to occupy ecological niches that would
11 otherwise be unavailable to them. Here we test this major evolutionary principle by
12 demonstrating self-organizing social behaviour in the plant-animal, *Symsagittifera*
13 *roscoffensis*. These marine aceol flat worms rely for all of their nutrition on the algae
14 within their bodies: hence their common name. We show that individual worms
15 interact with one another to co-ordinate their movements so that even at low
16 densities they begin to swim in small polarized groups and at increasing densities
17 such flotillas turn into circular mills. We use computer simulations to: (1) determine if
18 real worms interact socially by comparing them with virtual worms that do not interact
19 and (2) show that the social phase transitions of the real worms can occur based
20 only on local interactions between and among them. We hypothesize that such
21 social behaviour helps the worms to form the dense biofilms or mats observed on
22 certain sun-exposed sandy beaches in the upper intertidal of the East Atlantic and to
23 become in effect a super-organismic seaweed in a habitat where macro-algal
24 seaweeds cannot anchor themselves. *S. roscoffensis*, a model organism in many
25 other areas in biology (including stem cell regeneration), also seems to be an ideal
26 model for understanding how individual behaviours can lead, through collective
27 movement, to social assemblages.

28 **1. Introduction**

29 The study of collective motion is rapidly becoming a major interdisciplinary field in its
30 own right, bringing approaches from statistical physics to social behaviour [1]. This
31 field, at its best, is characterized by cycles of modelling and experimentation on
32 particular study systems that elucidate general principles applicable to, for example,
33 shaken metallic rods through macromolecules, bacterial colonies, amoebae, cells,
34 insects, fish, birds, mammals and human social behaviour [1]. One emergent
35 concept in the field of collective motion is that with increasing density many flocking
36 systems exhibit a series of phase transitions ranging from isolated individuals
37 through small polarized groups to circular mills and finally static assemblages. In
38 colloids and granular materials, the slowdown of movement with increasing density is
39 known as jamming [2], a transition also observed in human panic evacuation [3].
40 Systems that exhibit all three of these phase transitions are, however, rare (but see
41 recent work focussing on the last of these transitions in collective cellular movement
42 during metazoan development [4] and reticulate pattern formation in cyanobacteria
43 [5]). Here we test the idea that a new model system exhibits all three transitions.

44 Our study model is the marine flat aceol [6] worm *Symsagittifera roscoffensis*
45 renowned as the plant-animal [7],[8]. Adult *S. roscoffensis* feed on the nutrients
46 produced by the photosynthesizing symbiotic algae living within their bodies. Hence,
47 they seek sites where their algae can photosynthesize [9] more effectively. These
48 worms are typically encountered as biofilms on sandy beaches at low tide [8]. In
49 initial observations of *S. roscoffensis* transferred at fairly high densities to petri
50 dishes with a shallow pool of sea water, we noted a rapid and spontaneous
51 emergence of circular milling behaviour, which, to the best of our knowledge, had not

52 been described before in these worms, very possibly because it may occur only
53 fleetingly at a certain stage of the tidal cycle, for example when *S. roscoffensis*
54 initially come to the surface on the beaches they inhabit. Hence, the purpose of this
55 paper is to test hypotheses, through cycles of experimentation and modelling, which
56 focus on the transitions in the social behaviour and collective motion of these worms.
57 We determine how individual worms move, how small groups of worms interact with
58 one another and how circular mills form. We propose that circular milling gathers
59 worms together and eventually leads to such high densities that the worms can form
60 continuous biofilms and thus act as if they are a super-organismic seaweed.

61 One of the most extreme manifestations of collective motion is circular milling. It
62 occurs when individuals in a group are so synchronized that they follow one another
63 nose-to-tail in a complete ring in such a way that their trajectories are almost
64 identical and approximately circular; often there are multiple orbits nested within one
65 another [10],[11]. At the outset of modern studies of collective decision-making,
66 circular milling behaviour was seen as a key characteristic of ultra-cohesive group
67 movement [10]. It has been reported, for example, in *Bacillus* bacteria [12],[13] ,
68 *Daphnia* [14], processionary caterpillars [15], army ants [16], fish [17],[18] and
69 tadpoles [19]. Mechanistically, circular milling typically occurs because an isolated
70 group of individuals follow one another in a continuous ring. In processionary
71 caterpillars and army ants, circular milling is underpinned by individuals laying trails
72 that others follow and reinforce [15],[16]. In fish, it occurs because of rules of
73 attraction and alignment [11],[20],[21],[22]. A recent sophisticated analysis of
74 collective motion in glass prawns demonstrates that a weak form of circular milling
75 can occur in an annular arena because these supposedly non-social Crustacea
76 influence one another's movements even after a substantial delay following an

77 encounter [23].

78 The functional significance of circular milling is much less clear. Indeed, circular
79 milling seems often to be maladaptive, especially in processionary caterpillars and
80 army ants where individuals may remain trapped in a mill, by more and more trail
81 laying, until they die of exhaustion [16]. In fish, where it occurs fairly frequently, it
82 may serve for predator avoidance [20] through an extreme form of the geometry for
83 the selfish herd [24]. By contrast, in glass prawns, confinement to a donut-shaped
84 environment facilitates interactions and generates collective circular motion [23]. In
85 general, however, explanations for circular milling remain elusive. The experimental
86 tractability of the social behaviour and collective motion in *S. roscoffensis* we
87 demonstrate here, promises to elucidate the reasons why circular milling occurs both
88 mechanistically and functionally in this species.

89 First, we examine the characteristics of individual worms including their sizes, their
90 speeds of movement and their behavioural lateralization. Second, we determine if
91 these worms have a tendency to interact even at low densities such that they
92 encounter and line up with one another more frequently than they would if oblivious
93 of others. To do this, we create the first of two computer simulation models to mimic
94 the densities, lengths, and rates of movement of real worms in arenas of the same
95 size and shape as used in our experiments with real worms. This first model
96 represents the null hypothesis of no social interaction. Hence, we use simulations of
97 this model to detect potential social behaviours among the real worms. Third, we
98 analyse the occurrence of circular milling as a function of worm density. Fourth,
99 having established through comparisons with the null-hypothesis model that real
100 worms do interact socially, even at low densities, we create the second model based

101 on worms having simple rules of local interactions. The simulations of this second
102 model reproduce the formation of small polarized groups of moving worms that lead,
103 at yet higher densities, to circular mills. Finally, we put forward the hypothesis that
104 the purpose of these circular mills is to enable the worms to congregate into
105 extremely high-density assemblages that then can become biofilms.

106 **2. Material and methods**

107 **(a) Study organisms and experimental videos**

108 We collected *S. roscoffensis* from a north-easterly-facing beach on the North East
109 Coast of Guernsey on 17th to 19th June 2014. The worms were held at ambient
110 temperature in seawater collected from the same site and transferred to arenas for
111 filming. The depth of water within each arena was approximately 2 mm and the
112 worms were swimming freely. Filming at 15fps with a Canon G7 camera using a
113 resolution of 768 by 1024 pixels per frame followed within minutes of collection to
114 minimise the length of time the worms were held. We made fourteen videos of a total
115 of 707 worms. Thirteen of the videos recorded the behaviour of between 3 and 99
116 worms in a circular ceramic arena (2875mm²) for varying values at low density and
117 one recorded 293 worms in a square plastic weighing boat (961mm²) for a high-
118 density value. The videos were between 164 and 792s in length.

119 **(b) Characteristics of individual worms**

120 For length measurements, we took still images, in which each worm could be seen
121 clearly, from a representative sample from four of the videos at low worm densities in
122 the circular arenas (excluding two videos with 61 and 99 worms). Using ImageJ
123 software [25] a straight line was drawn across the diameter of the arena in each

124 image to provide a length calibration. We then used the ‘segmented line’ freehand
125 drawing tool, and the ‘fit spline’ option to draw a line from end to end of the worm,
126 matching any curvature, to produce a data set of worm lengths in mm.

127 For individual trajectories, we tracked worms in their quasi-2D environment of a
128 shallow pool of seawater in other four videos at low density in the circular arenas
129 using the AnTracks software system [26]. From these trajectories we extracted
130 length, speed, curvature and handedness to test for any relationship between length
131 and speed, explore the effect of curvature on speed and investigate whether
132 individual behavioural lateralization influences the formation of circular mills.

133 **(c) Interactions between worms: frequency**

134 We used the same interval of 2s (see later for justification) for the analysis of the
135 videos and their paired simulations to minimize any issues of pseudo-replication. As
136 the speeds of the worms in the videos and in the simulations were similar, the
137 chance that the same interactions would be seen in successive frames would be
138 similar, all else being equal, in both the videos and the simulations. Rather than
139 using automated methods to detect worm encounters in the simulations, we used the
140 same human observers to detect interactions both in the simulations and in the
141 experimental videos. It was not difficult for a human observer to count the well-
142 defined crossing and polarization events (see later) on still video frames and
143 simulation bitmap images. Hence, this very simple procedure ensured that the same
144 criteria were applied to both and hence that the difference between them was
145 reproducible.

146 *(i) Experimental videos*

147 The software 'ImageGrab' (<http://imagegrab.en.softonic.com/>, accessed October
148 2014) was used to take a still image from the videos every 2s. This interval was
149 chosen to avoid counting the same interaction twice because in 2s worms on
150 average moved approximately two body lengths (average length = 1.68mm, see
151 Results; average speed = 1.78mms^{-1} , see figure S1). The images were then
152 analysed one by one for the number of interactions. We recognized two types of
153 interaction: (1) crossing – two worms are in direct contact but are not aligned in the
154 same direction, that is, one is crossing over the other (the vertical proximity is
155 approximately 1mm, given the approximately 0.5 mm diameter of the worms and the
156 2mm water depth); (2) polarization – two worms are swimming in the same direction
157 and orientation, in close proximity (within 1mm), and in parallel or tandem positions.
158 Such close proximity (within 1mm) is almost certain to involve interaction even if only
159 owing to disturbance in the physical environment.

160 Each contact between any two or more worms was counted. Therefore, if a worm
161 had a worm parallel to it on either side, two polarized interactions were counted;
162 similarly if there were two worms swimming next to each other, and one was also
163 crossing over with a third worm, one crossing and one polarization interaction were
164 recorded. The total number of each interaction type was counted for each video and
165 then divided by the number of analysed images to calculate an average number of
166 interactions per image for a video. The analysis was based on 11 videos (figure
167 1c&d). The videos of the circular arena with 61 and 99 worms and of the square
168 arena with 293 worms were not included because such high densities made these
169 observations more difficult.

170 *(ii) Simulation of non-interacting worms*

171 The swimming behaviour of individual *S. roscoffensis* worms was recreated by
172 computer simulation. The scale of the simulation was the same as that of the
173 experimental video and the number of worms, and their lengths, were chosen to
174 match specific videos. The worms were made up of 0.2mm units, which moved
175 through the removal of a unit at the tail end and the replacement of it at the head
176 end, each time changing the head-end angle by up to +/- 0.1 rad using a uniform
177 distribution.

178 The simulation was configured so that it would run for the same length of time as the
179 corresponding video and had an option to save bitmaps at set intervals. This function
180 was used to collect the screenshots that were analysed. The worms were produced
181 in six colours, and had a black dot at the leading or 'head' end to aid in identifying the
182 direction of movement during analysis (e.g. to determine polarized events).

183 The simulation used realistic worm lengths and densities to replicate each video. The
184 bitmap interval was set to 2s and the number of frames entered so that the
185 simulation run time would match the duration of each video as in **(c)** (i).

186 For each image the number of crossings and polarization events were recorded, the
187 different colours of the worms aided counting the number of worms involved in each
188 event, and the black heads helped to differentiate between parallel worms travelling
189 in the same and different directions. The total number of events was then divided by
190 the number of images as in the video analysis.

191 **(d) Interactions between worms: duration**

192 (i) *Experimental videos*

193 We calculated the mean duration of polarization interactions for each of the 11
194 videos also analysed for interaction frequency. We analysed a maximum of 20 such
195 interactions from each video. A random number generator was used to select 20 if
196 more had been recorded. The video was restarted at the beginning of each
197 interaction and followed through to its end. We calculated each interaction duration
198 as the difference between its start and end frame number.

199 *(ii) Simulation of non-interacting worms*

200 We mimicked the procedure with the videos of real worms as described in **(d)** *(i)* with
201 simulations of non-interacting worms. We scrolled through the bitmaps until
202 polarization events were found, and then followed the event from the first to the last
203 image in which it occurred. The number of bitmaps featuring the event was used to
204 produce the event duration in seconds based on the bitmap interval of 500ms. We
205 thus found the mean event duration for the simulation corresponding to each video.

206 **(e) Interactions between worms: aggregation formation**

207 *(i) Experimental videos*

208 We analysed all 14 videos to examine worm clustering (figure 1e). Using ImageGrab
209 we took a screenshot from the videos every 20s. In each image the number of
210 clusters was counted. We defined clusters as occurring when two or more worms
211 were in direct contact.

212 *(ii) Simulation of non-interacting worms*

213 The cluster counts for the simulation were performed by a modified version of the
214 simulation program. The bitmaps of the simulation at 20s intervals were loaded and
215 then the programme counted the number of clusters per bitmap.

216 **(f) Circular milling as a function of density**

217 The presence or absence of circular milling was recorded in 100 x 100mm petri
218 dishes. Five were used for each of 17 dilution series making up 85 data points
219 altogether for density. The worms were pipetted with sea water into a plastic beaker
220 to produce a high density of *S. roscoffensis* worms in approximately 50ml of water.
221 This was enough to complete one dilution series as follows: 8ml was pipetted into
222 the first petri dish and then 4ml, 2ml, 1ml and 0.5ml into the second to fifth petri dish,
223 respectively. The mixture in the beaker was consistently and evenly stirred
224 throughout the pipetting process to ensure the mixture of *S. roscoffensis* and sea
225 water was as homogeneous as possible. Sea water collected from the habitat of *S.*
226 *roscoffensis* was then added to each petri dish to make the total volume of water in
227 each up to 40ml. At time zero all of the petri dishes were agitated to ensure that
228 there were no mills present at the beginning of the experiment.

229 We observed the group of petri dishes for 60min and recorded the presence or
230 absence of circular mills in each during that period. If a circular mill was seen, further
231 observation of that petri dish ceased at that time. Thus for each of the 85 density
232 values we recorded a value of 1 if at least one mill formed and a value of 0 if no mills
233 formed over the 60min-period of observation. At the end of the observations a
234 photograph was taken of the most dilute dish of each series and the number of *S.*
235 *roscoffensis* worms was counted with ImageJ. The numbers in the other petri dishes
236 were estimated from the number counted in the most dilute dish.

237 With worms collected at the same field site as described above but in June 2015, we
 238 studied the directionality of circular milling by again video-recording them in plastic
 239 arenas. These data were also used in our analysis of the possible effect of arena
 240 walls on the formation of circular mills (figure S5).

241 **(g) Simulation of interacting worms**

242 The simulation took place in a circular arena containing $N \leq 10000$ worms placed
 243 initially at random. Each worm consisted of a pair of jointed rods each 5 units long
 244 with an angle between them up to ± 0.05 rad. At fixed time intervals dt the worm
 245 was advanced by a distance $s = v dt (1 - gc)$ along its circumscribed circle, where v
 246 was the worm's standard straight-line speed, c its instantaneous curvature and g a
 247 constant describing how the worm slows when turning. The final angle of the head
 248 section was then chosen from the existing one and four alternative random
 249 directions within ± 0.15 rad of the tail direction and on the basis of which of these
 250 five options best accommodated the head with respect to the heads and tails of
 251 neighbouring worms.

252 For each candidate position of the head, we calculated the energy $U = \sum \lambda u(r)$ where
 253 the summation was taken with respect to the head and tail positions of all other
 254 worms within r_{\max} and r was the relevant separation (figure S4). We used an
 255 approximation of the Lennard-Jones model for pair-wise interaction (figure 3a), as
 256 commonly used in such simulations [1]:

$$\begin{aligned}
 257 \quad & u(r) = 1 - 2r/r_{\min} && r < r_{\min} \\
 258 \quad & = - (r_{\max} - r)/(r_{\max} - r_{\min}) && r_{\min} \leq r \leq r_{\max} \\
 259 \quad & = 0.0 && r > r_{\max}
 \end{aligned}$$

260 The multiplier λ took the value 1.0 for head-tail calculations. For head-head

261 calculations we used $\lambda = 0.5$ if the tails of the two worms were separated by more
262 than the length of a worm, otherwise $\lambda = 2.0$. This weighting factor favoured
263 polarized (head-to-head) alignment. The lowest of these energies was adopted for
264 the new head position.

265 After each set of recalculations, the worms' identification numbers were shuffled to
266 avoid undue influence by any one of them, and a simple reflection procedure
267 ensured that worms stayed within the arena.

268 The values adopted for the various constants had been based where possible on
269 measurements on real worms and translated into the artificial arena (figure S4).

270 The circular arena had a radius of 200 units and given that the virtual and real worms
271 had a length of 10 units and on average 1.68mm, respectively, this represented an
272 arena of radius 33.6mm and an area of 3547mm².

273 We used the same simulation model in our analysis of the effect of arena boundaries
274 on the formation of circular mills (figure S5).

275 **3. Results**

276 **(a) Characteristics of individual worms**

277 The worms in our samples had a mean length of 1.68mm (SE = 0.075mm, N=57)
278 with the smallest being 0.54mm and the largest 2.91mm long. Their speed was well
279 within the distribution measured by other methods in earlier studies [9]. It increased
280 significantly with length but rather weakly and there was much variation (figure S1).
281 At low density in the circular arenas, the convoluted trajectories of individual worms
282 (figure 1a) were significantly biased towards clockwise movements (33 in a sample

283 of 41, Binomial two-tailed test, $p = 0.0001$; figure S2). Their speed declined markedly
284 as a function of body curvature (figure S3a,b) which in turn set their future
285 trajectories (figure 1a).

286 **(b) Interactions between worms**

287 To test if the worms have a tendency to interact with one another, we compared the
288 paired videos of the real worms and the simulations of non-interacting and non-
289 laterally-biased worms to determine if the real worms have either more or fewer
290 interactions than the purely random encounters of the simulated worms. This
291 comparison revealed that the real worms actively interact with one another even at
292 rather low densities (figure 1c).

293 We considered two or more worms to be potentially interacting, either in the
294 experimental videos or in the simulations, when they were less than 1mm apart.
295 Indeed, when this condition is met, typically the worms might be crossing over one
296 another or swimming in the same direction with their bodies in parallel (the latter
297 included worms that were closely following one another, as if in tandem). Such
298 parallel similarly orientated movement, either side by side or following, is known as
299 polarization [18].

300 The worms interacted with one another disproportionately more frequently as their
301 density increased (figure 1b). The durations of individual polarization events
302 increased with worm density among the real but not among the virtual worms in the
303 null model simulation (figure 1d). As densities increased, several of the worms
304 became involved in the same polarization interaction. In this way, they began to form
305 small cohesive fleets, which we call flotillas (figure 1b).

306 Real worms maintained contact with one another so frequently with increasing
307 densities that counting the number of isolated objects (single worms plus groups of
308 touching worms) in freeze frames of experimental videos vs. simulations showed a
309 significant difference in the numbers of observed discrete entities (figure 1e). In
310 short, there were significantly fewer (but bigger) aggregations among the real worms
311 than among the virtual worms because they associated more with increasing density.

312 **(c) Circular milling and directionality as a function of density**

313 The separate experiments with different densities of worms in the 100 x 100mm petri
314 dishes showed that the likelihood of circular milling in *S. roscoffensis* (figure 2a)
315 increases abruptly as a function of increasing density (figure 2b). When they began
316 to form, the initial diameter of these circular mills was on the order of about 10mm
317 and they were often well away from the dish edge (figure 2c). If anything, they are
318 more likely to form near the centre (figure S5). Thus, the circular milling of these
319 worms does not occur because they are responding to the boundaries of their arena
320 as a template; rather they occur because the worms are influencing one another's
321 movements.

322 Our observations from June 2015 showed that out of 45 circular mills all but one
323 were clockwise.

324 **(d) Simulation modelling of interacting worms**

325 *S. roscoffensis* worms may only be able to detect one another at very short
326 distances. Hence, we produced a new computer simulation of these worms'
327 movements with only very local interactions between them (figures 3a & S4) to
328 determine how the observed phase transitions, that is from solitary worms, to

329 polarized flotillas, to large circular mills might occur through self-organization [17].
330 Because we knew the size and speed of the real worms (figure S1) and the effect of
331 curvature on their speeds (figure S3), there were few arbitrary parameters. We
332 observed flotillas and milling (figure 3b) with reasonable choices for the elapsed time
333 per iteration, the maximum range of any interaction and the separation at which the
334 potential energy is at a minimum (figures 3a & S4). The likelihood of milling after a
335 given time interval as a function of N (figure 3c) was similar qualitatively to the
336 experimental data (figure 2b).

337 The behavioural lateralization of individual worms is likely to promote the probability
338 of circular milling at lower densities (figure 3c).

339 **4. Discussion**

340 Through cycles of experimentation and modelling we have been able to demonstrate
341 how individual worms move at low densities, how they begin to interact with one
342 another and how with increasing density this leads to circular milling behaviour.

343 The worms propel themselves through the action of cilia on their surface. However,
344 they also have muscles that determine the curvature of their bodies and hence the
345 curvature of their trajectories [8]. Such small average changes in speed with length
346 may occur because drag will be proportional to surface area, as is the number of
347 cilia, whose combined power combats such drag [27]. This might explain why worms
348 of different sizes, but all of similar proportions, move at surprisingly similar speeds.

349 Clearly, the behaviours leading to circular mill formation begin to be seen even at
350 fairly low densities; namely worms influencing one another's movements to form
351 lasting parallel formations and aggregations. Such social behaviour becomes ever

352 more common with increasing worm density (figure 2*b*).

353 The rather constant average speeds of the worms, despite substantial differences in
354 body lengths (figure S1), and their tendencies to turn in the same clockwise
355 directions (figure S2) seem to be adaptations that favour circular milling (figure 3*c*).
356 Individual worms exhibit behavioural lateralization such that they move in a
357 clockwise direction; the vast majority of circular mills (44 of the 45 observed in 2015)
358 have a clockwise rotation and simulations show that circular milling will occur at
359 lower densities when individual worms have the same directional biases.

360 In contrast to other organisms, such as starlings [28],[29], that show collective group
361 movements, these worms may only be able to detect one another at very short
362 distances and hence our simulations of potentially interacting worms are based only
363 on relatively local interactions between the worms. These simulations replicate the
364 circular milling seen among the real worms at relatively high densities (figure 3*b,c*).
365 Thus we have been able to establish how the movements of, and simple local
366 interactions between, individuals contribute to the self-organizing emergent
367 properties and phase transitions of large groups [17].

368 So far we have examined what factors favour circular milling in these plant-animals
369 from a mechanistic view point. Now we will consider its possible adaptive value.
370 Circular milling appears to be maladaptive in army ants and processionary
371 caterpillars. Furthermore, in the non-social glass prawns, where it arises under
372 environmental conditions which facilitate interaction during motion around a ring, it
373 also seems to serve no apparent purpose [23]. However, we hypothesize that, where
374 they are adaptive, circular mills may act as a positive-feedback vortex to capture the
375 highest possible local densities of organisms for protection by numbers or other

376 social advantages. In the case of *S. roscoffensis* considered here circular milling
377 may enable these plant-animals to form very dense biofilms or mats that allow them
378 to behave collectively as a social seaweed and colonize sandy beaches (figure
379 4a&b) where traditional macro-algal seaweeds would be unable to anchor a holdfast.
380 We hypothesize these mats enable the worms to stabilize their positions in pools of
381 seepage sea water on sandy beaches (figure 4b), by sharing a more or less
382 continuous mucous sheath. The sharing of such a relatively thick mucous sheet may
383 also enable the worms to benefit from sunlight on both of their sides at once as their
384 underside receives solar energy reflected from the substrate [8].

385 Recently it has been shown that individual *S. roscoffensis* worms move towards light
386 intensities that may be detrimental to the maximum photosynthetic rates of their
387 symbiotic algae [9]. Our findings here may help to resolve this paradox because
388 these worms are very likely to form dense aggregates at high light intensities and
389 may take it in turns to be sheltered or exposed by burrowing inside or onto the
390 surface of such social conglomerates. Such behaviour, using conspecific
391 aggregations as living shields against environmental extremes, is seen, for example,
392 in Emperor Penguins who form rotating huddles as protection against extreme
393 Antarctic winds [30], [31]. The worms are likely to find greater individual safety in
394 these hugely dense aggregations and may even be able to defend themselves
395 collectively through the mass production of dimethylsulphoniopropionate (DMSP)
396 [8],[32],[33].

397 Our demonstration of social behaviour, with multiple phase transitions, in *S.*
398 *roscoffensis* fills a missing tier in the long list of organisms in which collective motion
399 has been observed [34], [1]. We confidently predict that the diversity of organisms

400 exhibiting social collective motion, at all levels of biological complexity, will continue
401 to grow for the foreseeable future and that the importance of social behaviour as a
402 major evolutionary transition [35] will be increasingly recognized.

403 **Ethics**

404 All *S. roscoffensis* worms were returned to the place on the shore from where they
405 were collected after the experiments.

406 **Data accessibility**

407 All data associated with this paper can be found at the designated Dryad depository:
408 doi:10.5061/dryad.1n70s

409 **Authors' contributions**

410 N.R.F. initiated and designed the study, A.W. conducted the modelling, K.A.J.G. and
411 A.R.G. carried out the experiments, V.V. and H.P. analysed the experimental videos,
412 C.D. and M.L.G. helped with the experiments, M.C.S. provided the tracking software,
413 A.B.S.F. carried out the statistical analysis. N.R.F, A.W. and A.B.S.F. drafted the
414 paper. All authors contributed to revisions.

415 **Competing interests**

416 We declare we have no competing interests.

417 **Funding**

418 We received no funding for this study.

419 **Acknowledgments**

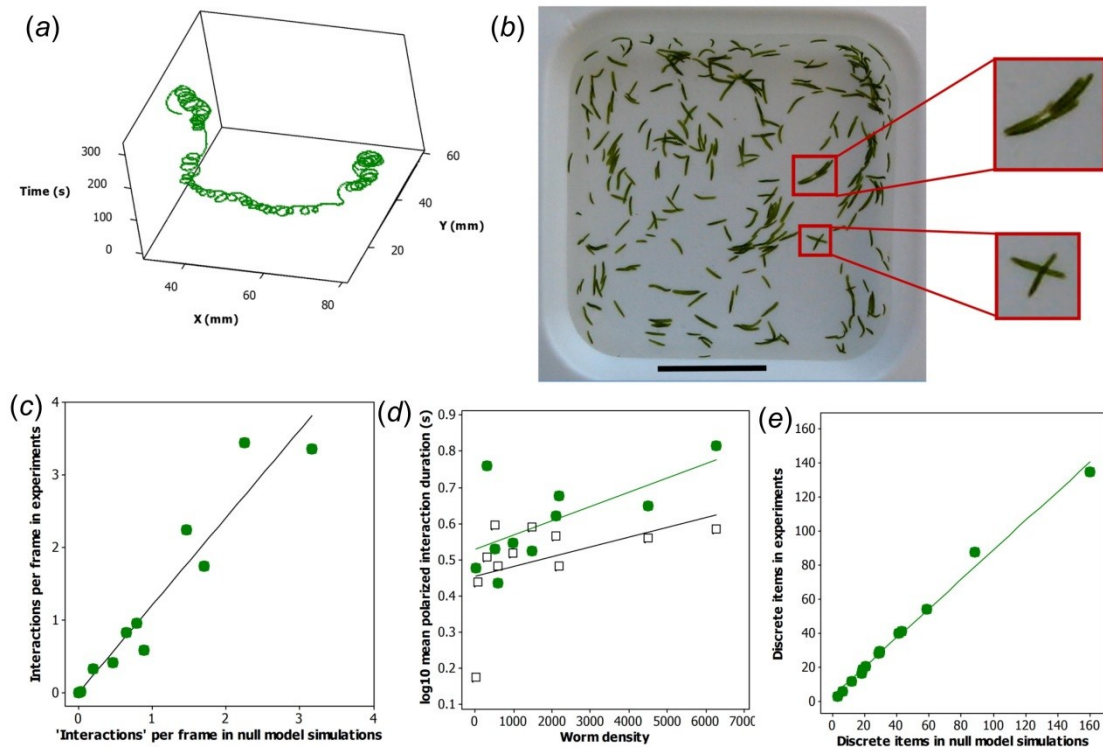
420 We wish to thank Ann Coquelin for her help and kindness in providing facilities for our work
421 in Guernsey. We gratefully acknowledge two anonymous referees for their helpful
422 comments.

423 **References**

- 424 1. Vicsek, T. & Zafeiris, A. 2012 Collective motion. *Phys. Rep.* **517**, 71–140.
 425 (doi:10.1016/j.physrep.2012.03.004)
- 426 2. Biroli, G. 2007 Jamming: A new kind of phase transition? *Nat. Phys.* **3**, 222–
 427 223. (doi:10.1038/nphys580)
- 428 3. Helbing, D., Farkas, I. J. & Vicsek, T. 2000 Simulating dynamical features of
 429 escape panic. *Nature* **407**, 487–490. (doi:10.1038/35035023)
- 430 4. Sadati, M., Taheri Qazvini, N., Krishnan, R., Park, C. Y. & Fredberg, J. J. 2013
 431 Collective migration and cell jamming. *Differentiation*. **86**, 121–5.
 432 (doi:10.1016/j.diff.2013.02.005)
- 433 5. Tamulonis, C. & Kaandorp, J. 2014 A Model of Filamentous Cyanobacteria
 434 Leading to Reticulate Pattern Formation. *Life* **4**, 433–456.
 435 (doi:10.3390/life4030433)
- 436 6. Boutilier, S. J. & Hejnol, A. 2009 Acoels. *Curr. Biol.* **19**, R279–R280.
 437 (doi:10.1016/j.cub.2009.02.045)
- 438 7. Keeble, F. 1910 *Plant-Animals: a Study in Symbiosis*. Cambridge: Cambridge
 439 University Press.
- 440 8. Bailly, X. et al. 2014 The chimerical and multifaceted marine acoel
 441 Symsagittifera roscoffensis: from photosymbiosis to brain regeneration. *Front.*
 442 *Microbiol.* **5**, 1–13. (doi:10.3389/fmicb.2014.00498)
- 443 9. Nissen, M., Shcherbakov, D., Heyer, A., Brummer, F. & Schill, R. O. 2015
 444 Behaviour of the plathelminth Symsagittifera roscoffensis under different light
 445 conditions and the consequences for the symbiotic algae Tetraselmis
 446 convolutae. *J. Exp. Biol.* **218**, 1693–1698. (doi:10.1242/jeb.110429)
- 447 10. Deneubourg, J. L. & Goss, S. 1989 Collective patterns and decision-making.
 448 *Ethol. Ecol. Evol.* **1**, 295–311. (doi:10.1080/08927014.1989.9525500)
- 449 11. Lukeman, R., Li, Y. X. & Edelstein-Keshet, L. 2009 A conceptual model for
 450 milling formations in biological aggregates. *Bull. Math. Biol.* **71**, 352–382.
 451 (doi:10.1007/s11538-008-9365-7)
- 452 12. Ben-Jacob, E., Cohen, I., Czirók, A., Vicsek, T. & Gutnick, D. L. 1997
 453 Chemomodulation of cellular movement, collective formation of vortices by
 454 swarming bacteria, and colonial development. *Phys. A Stat. Mech. its Appl.*
 455 **238**, 181–197. (doi:10.1016/S0378-4371(96)00457-8)
- 456 13. Sokolov, A., Apodaca, M. M., Grzybowski, B. A. & Aranson, I. S. 2010
 457 Swimming bacteria power microscopic gears. *Proc. Natl. Acad. Sci. U. S. A.*
 458 **107**, 969–974. (doi:10.1073/pnas.0913015107)
- 459 14. Ordemann, A., Balazsi, G., Caspari, E. & Moss, F. 2003 Daphnia swarms: from
 460 single agent dynamics to collective vortex formation. In *SPIE's First ...*, pp.

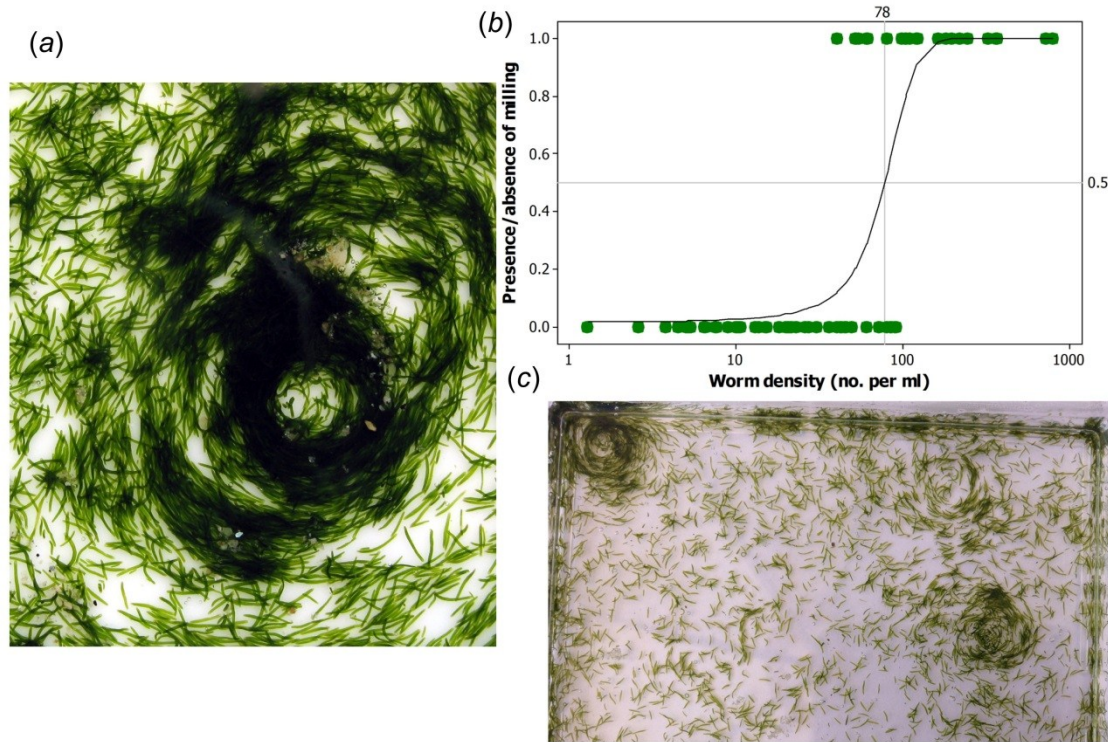
- 461 172–179.(doi:10.1117/12.489033)
- 462 15. Fabre Jean-Henri & Legros Georges Victor 1879 *Souvenirs entomologiques : études sur l'instinct et les moeurs des insectes / J.-H. Fabre*. Paris: Marie
463 Léonard.
464
- 465 16. Franks, N. R., Gomez, N., Goss, S. & Deneubourg, J. L. 1991 The blind
466 leading the blind in army ant raid patterns: Testing a model of self-organization
467 (Hymenoptera: Formicidae). *J. Insect Behav.* **4**, 583–607.
468 (doi:10.1007/BF01048072)
- 469 17. Camazine, S., Deneubourg, J. L., Franks, N. R., Sneyd, N. R., Theraulaz, G. &
470 Bonabeau, E. 2001 *Self-organization in biological systems (Princeton Studies in Complexity)*. Princeton: Princeton University Press.
471
- 472 18. Soria, M., Freon, P. & Chabanet, P. 2007 Schooling properties of an obligate
473 and a facultative fish species. *J. Fish Biol.* **71**, 1257–1269. (doi:10.1111/j.1095-
474 8649.2007.01554.x)
- 475 19. Bazazi, S., Pfennig, K. S., Handegard, N. O. & Couzin, I. D. 2012 Vortex
476 formation and foraging in polyphenic spadefoot toad tadpoles. *Behav. Ecol. Sociobiol.* **66**, 879–889. (doi:10.1007/s00265-012-1336-1)
477
- 478 20. Couzin, I. D., Krause, J., James, R., Ruxton, G. D. & Franks, N. R. 2002
479 Collective memory and spatial sorting in animal groups. *J. Theor. Biol.* **218**, 1–
480 11. (doi:10.1006/jtbi.3065)
- 481 21. Couzin, I. D., Krause, J., Franks, N. R. & Levin, S. A. 2005 Effective leadership
482 and decision-making in animal groups on the move. *Nature* **433**, 513–516.
483 (doi:10.1038/nature03236)
- 484 22. Calovi, D. S., Lopez, U., Ngo, S., Sire, C., Chaté, H. & Theraulaz, G. 2014
485 Swarming, schooling, milling: Phase diagram of a data-driven fish school
486 model. *New J. Phys.* **16**. (doi:10.1088/1367-2630/16/1/015026)
- 487 23. Mann, R. P., Perna, A., Strömbom, D., Garnett, R., Herbert-Read, J. E.,
488 Sumpter, D. J. T. & Ward, A. J. W. 2013 Multi-scale inference of interaction
489 rules in animal groups using Bayesian model selection. *PLoS Comput. Biol.* **9**,
490 e1002961. (doi:10.1371/journal.pcbi.1002961)
- 491 24. Hamilton, W. D. 1971 Geometry for the selfish herd. *J. Theor. Biol.* **31**, 295–
492 311. (doi:10.1016/0022-5193(71)90189-5)
- 493 25. Schneider, C. A., Rasband, W. S. & Eliceiri, K. W. 2012 NIH Image to ImageJ:
494 25 years of image analysis. *Nat. Methods* **9**, 671–675.
495 (doi:10.1038/nmeth.2089)
- 496 26. Stumpe, M. 2012 AnTracks.
- 497 27. Alexander, R. M. 1970 *Functional design in fishes*. London: Hutchinson
498 University Library.
- 499 28. Cavagna, A., Cimarelli, A., Giardina, I., Parisi, G., Santagati, R., Stefanini, F. &
500 Viale, M. 2010 Scale-free correlations in starling flocks. *Proc. Natl. Acad. Sci. U. S. A.* **107**, 11865–11870. (doi:10.1073/pnas.1005766107)
501

- 502 29. Pearce, D. J. G., Miller, A. M., Rowlands, G. & Turner, M. S. 2014 Role of
503 projection in the control of bird flocks. *Proc. Natl. Acad. Sci.* **111**, 10422–
504 10426. (doi:10.1073/pnas.1402202111)
- 505 30. Ancel, A., Visser, H., Handrich, Y., Masman, D. & Maho, Y. Le 1997 Energy
506 saving in huddling penguins. *Nature*. **385**, 304–305. (doi:10.1038/385304a0)
- 507 31. Gerum, R. C., Fabry, B., Metzner, C., Beaulieu, M., Ancel, a. & Zitterbart, D. P.
508 2013 The origin of traveling waves in an emperor penguin huddle. *New J.*
509 *Phys.* **15**. (doi:10.1088/1367-2630/15/12/125022)
- 510 32. Raina, J.-B. et al. 2013 DMSP biosynthesis by an animal and its role in coral
511 thermal stress response. *Nature* **502**, 677–80. (doi:10.1038/nature12677)
- 512 33. Wolfe, G. V, Steinke, M. & Kirst, G. O. 1997 Grazing-activated chemical
513 defence in a unicellular marine alga. *Nat.* **387**, 894–897. (doi:10.1038/43168)
- 514 34. Sumpter, D. J. T. 2010 *Collective animal behaviour*. Princeton University Press.
- 515 35. Maynard Smith, J. & Szathmary, E. 1995 *The major transitions in evolution*.
516 Oxford University Press.
- 517
518

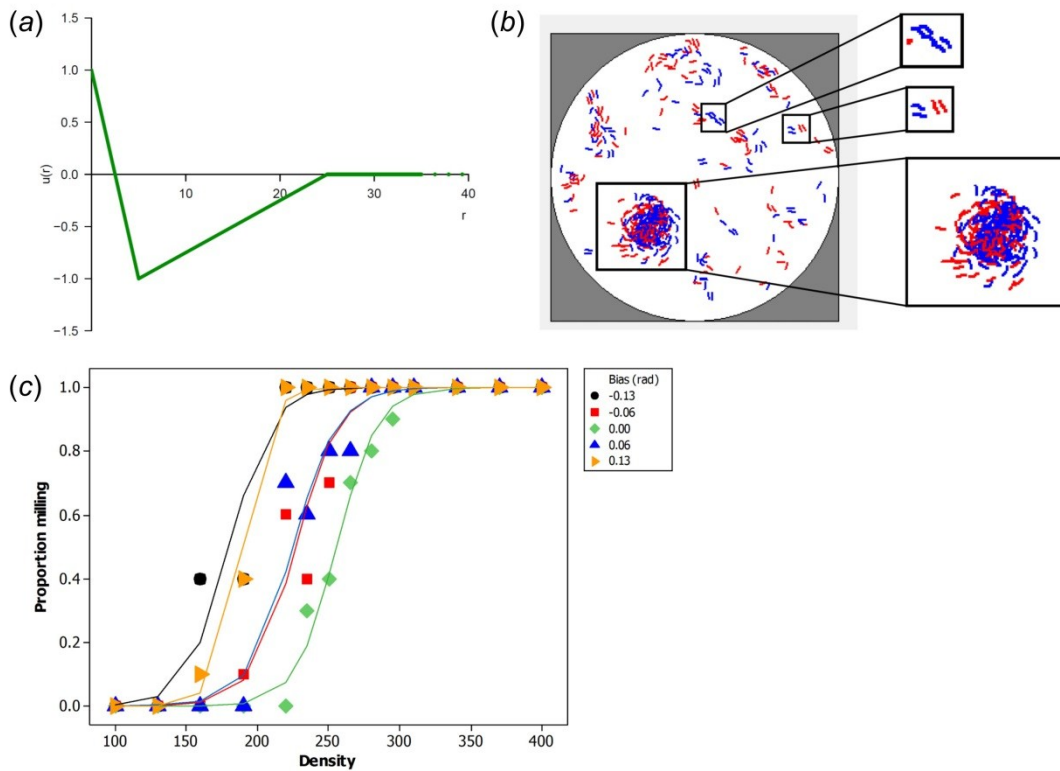


519
520 **Figure 1.** Movement of individual *S. roscoffensis* worms and behaviour at
521 intermediate densities. (a) Convoluted trajectory of a single worm. This individual
522 made predominantly clockwise movements. (b) Flotilla formation at intermediate
523 densities. The black scale bar at the bottom of the arena represents 10mm. The
524 upper red square shows a polarized group of 4 worms moving in the same direction
525 in mutual contact (i.e. a flotilla; see also the upper panel to the right). The lower red
526 square shows two worms crossing over one another (see also the lower panel to the
527 right). (c) Comparison between number of interactions (per frame, both crossings
528 and polarizations, see Material and methods) among worms in experimental videos
529 and number of crossing and polarization events (per frame) in paired null model
530 simulations at low to intermediate densities. The line of best fit passes through the
531 origin and has a slope = 1.205 ($t_9 = 15.44$, $p < 0.001$), which is significantly greater
532 than 1 (95% CI: 1.029, 1.381; see ESM). Thus, there are more interactions between
533 the real than between the virtual worms. (d) Polarized interaction durations increased
534 among real worms in the experiments (green circles) but not among the virtual
535 worms in the null model simulations (empty squares) which are paired with each
536 experimental video (N=11). The gradient of the relationship between \log_{10} mean
537 polarization event duration (s) and worm density is significantly different from 0 for
538 the videos (slope = 0.000040, $t_8 = 2.44$, $p = 0.040$), but not for the null model
539 simulations (slope = 0.000027, $t_9 = 1.53$, $p = 0.161$). This means that the relationship
540 between polarization event duration and density (see ESM) can be attributed entirely
541 to the data from the worms in the experiments. (e) The worms aggregate more in the
542 experimental videos than in the null model simulations with increasing density as
543 shown by the slope of the regression line being significantly less than 1. (N=14; data
544 from 13 circular arenas and 1 densely populated square arena (the latter is
545 represented by the point at the top right.) Thus there are fewer discrete objects in the
546 videos than in the paired null model simulations. The equation of the line is: No. of

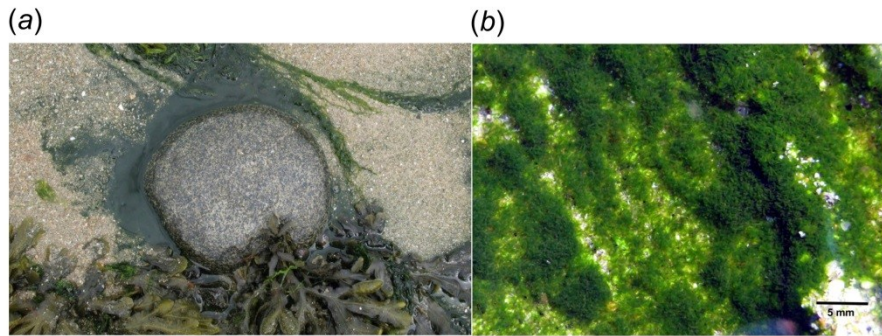
547 discrete items in experiments = $3.19 + 0.858$ No. of discrete items in simulations (R^2
 548 = 99.2%). The slope is significantly different from 0 ($t_{12} = 38.73$, $p < 0.001$) and
 549 significantly smaller than 1 (95% CI: 0.810 - 0.906; 99% CI: 0.790 - 0.925; see ESM).
 550



551
 552 **Figure 2.** *S. roscoffensis* worms exhibit milling as a step function of increasing
 553 density. (a) A circular mill in a small arena. (b) The relationship between worm
 554 density (no. per ml) and the presence or absence of circular mills (1 and 0,
 555 respectively); green circles: data, black line: predicted probabilities from the fitted
 556 binary logistic regression model $\log(\pi/(1-\pi)) = -4.126 + 0.053x$, where π is the
 557 probability of milling and x is worm density. The model predicts that with every
 558 additional worm per ml the probability of milling increases on average by 5% (95%
 559 CI: 3 – 8%) and that at density above 78 worms/ml, the presence of milling becomes
 560 more likely than not (see ESM). (c) Part of a 100 x 100mm petri dish where three
 561 circular mills have formed.
 562



563
 564 **Figure 3.** Simulation of interacting worms. (a) Potential energy curve, an
 565 approximation of the Lennard-Jones model [1], used for pair-wise interactions in the
 566 simulation of interacting worms; $u(r)$: potential energy function, $u(r) > 0$: repulsion;
 567 $u(r) < 0$: attraction; r : range of interaction; at $r_{\min} = 5$ attraction is at its maximum and
 568 $r_{\max} = 25$ is the maximum range for any interaction (see figure S4 for pseudocode).
 569 (b) The results of one simulation showing one circular mill (lower panel) and several
 570 flotillas (examples in the top two sub-panels; worms in blue or red are temporarily
 571 moving clockwise or anticlockwise, respectively; note, these simulations have neither
 572 left nor right biases in the movements of individual worms). (c) Self-organizing
 573 circular mills in the simulations as a function of density for different levels of lateral
 574 bias (rad) in the movement of individual worms; the bias range -0.13 to 0.13 rad
 575 goes from clockwise to anticlockwise with 0.00 rad representing no bias. There was
 576 a significant effect of density on the proportion of simulations with milling (out of 10
 577 simulations for each value of density); note density here (i.e. the number of worms
 578 per simulation arena) cannot be directly compared to density of the real worms in a
 579 volume of sea water. For each of the five levels of bias, the proportion of simulations
 580 with milling increased by 7% (95% CI: 6 – 9%, $p < 0.001$, see ESM) with every
 581 additional worm. However, the inflection points differed; the inflection point for no
 582 bias (0.00 rad) was significantly different from the other four while the inflection
 583 points for clockwise and anticlockwise biases of the same magnitude (-0.13 and 0.13
 584 rad or -0.06 and 0.06 rad) were not significantly different from each other and
 585 significantly different from the rest (table S1).
 586



587
588 **Figure 4.** Dense mat formation of *S. roscoffensis* on a Guernsey beach. (a) The
589 worms are in the drainage channel (from 7 to 2 o'clock) around the circular rock
590 which is approximately 15cm across. The rock is an anchor for the holdfasts of the
591 macro-algae in the photograph, whereas the worms will burrow into the sand on the
592 incoming tide. (b) A close-up of a mat revealing heterogeneity in worm density.
593